Determination of the Ion Temperature in a Stainless Steel Slab Exposed to Intense Ultrashort Laser Pulses

E. Principi,[1,*] R. Cucini,[1] A. Filipponi,[2] A. Gessini,[1] F. Bencivenga,[1] F. D'Amico,[1] A. Di Cicco,[3,4] and C. Masciovecchio[1]

[1]*Sincrotrone Trieste S.C.p.A., S. S. 14 km 163.5, Area Science Park, 34149 Basovizza, Trieste, Italy*

[2]*Dipartimento di Scienze Fisiche e Chimiche, Università degli Studi dell'Aquila, Via Vetoio, 67100 L'Aquila, Italy*

[3]*CNISM, Scuola di Scienze e Tecnologie, Sezione di Fisica, Università di Camerino, 62032 Camerino (MC), Italy*

[4]*IMPMC-CNRS UMR 7590, Université P. et M. Curie, 4 place Jussieu, 75005 Paris, France*

(Received 4 January 2012; published 13 July 2012)

We present an effective approach to determine the amount of energy absorbed by solid samples exposed to ultrashort laser pulses, thus, retrieving the maximum temperature attained by the ion lattice in the picosecond time scale. The method is based on the pyrometric detection of a slow temperature fluctuation on the rear side of a sample slab associated with absorption of the laser pulse on the front side. This approach, successfully corroborated by theoretical calculations, can provide a robust and practical diagnostic tool for characterization of laser-generated warm dense matter.

DOI: 10.1103/PhysRevLett.109.025005 PACS numbers: 52.50.Jm, 41.60.Cr, 44.10.+i, 52.27.Gr

Nowadays, high-energy density subpicosecond pulsed lasers cover a broad spectrum of wavelengths ranging from the visible, domain of amplified pulsed lasers, to the extreme ultraviolet and x-ray regions, accessible by innovative single pass free electron laser (FEL) facilities. The direct interaction of such ultrafast lasers with solid specimens can generate, in a laboratory, unexplored states of matter that can be found in nature only in the astrophysical context [1,2], characterized by temperatures up to hundreds of eV [3] and pressures up to the Mbar regime [4]. Under those conditions, matter can appear as a dense plasma and exhibits properties still not entirely understood. The "warm dense matter" (WDM) [5] is an intriguing subset of laser-generated dense plasma lying between the condensed matter and the plasma domains, that has recently attracted much interest. WDM investigation is regarded as one of the grand challenges of contemporary physics [6] and its comprehension is expected to generate a profound impact in multidisciplinary scientific fields as well as in the technological one with a specific application to the inertial confinement fusion process [7]. For these reasons, great efforts have been devoted in the last years to the construction of experimental infrastructures, based on FEL large scale facilities, capable to both generate and analyze the WDM state.

WDM manifests itself after ultrafast heating of a solid sample as a consequence of the thermalization process of the electron and ion systems at temperatures from about 1 eV to several tens of eV. Contrary to a classical plasma, in WDM, both the ion and electron systems exhibit strong coupling resulting in a tangible atomic structural order. However, condensed matter theory does not assign any long range atomic order to the WDM state, its thermal energy being comparable with its Coulomb correlation energy. This ambiguity results in the lack of a reliable theoretical framework capable to predict the properties of the WDM regime. Significant difficulties for the study of WDM emerge also in the experimental approach. While it is relatively simple to generate WDM, many issues hinder its profitable investigation. For example, it is still not clear how and with what efficiency the laser energy is transferred to solid matter [8]. This drastically limits our ability to determine the thermodynamic state of laser-generated warm dense materials. In this sense, a great advantage of ultrafast direct laser heating is the possibility to deposit a huge amount of optical energy without affecting the density of the sample (isochoric heating). In these conditions, the density of the target can be assumed invariant [9], at least until the occurrence of significant hydrodynamic expansion expected to start a few picoseconds after WDM generation [10]. On the contrary, the absorbed energy and the sample temperature are experimental variables that must be measured. Typically, laser-generated WDM is characterized from the perspective of the plasma diagnostic. Consequently, the sample temperature is often associated with the temperature of its electron system estimated by means of soft-x-ray spectroscopy [11] or x-ray scattering [12–14]. However, as stated by the two-temperature model [10], in the picosecond time scale, the electron temperature (T_e) significantly exceeds the temperature of the ion system (T_i). In order to gain a robust characterization of the thermodynamic state of a warm dense sample excited by an intense fs laser, the knowledge of T_e should be complemented and corroborated by information on T_i.

In this Letter, we propose a practical and effective experimental approach to estimate the amount of absorbed energy (E_a) as well as the ion temperature (T_i) in laser- and FEL-generated WDM. Our method does not account for complicated absorption and emission processes and related transient phenomena occurring within the first 100–200 fs. In this time scale, the energy transfer is still limited to the

electron system leaving the ion system substantially unaltered. Within several picoseconds [9] after the absorption of the laser pulse, a fraction of the laser energy is effectively transferred to the ion system and subsequently diffused in the form of heat. We assume that heat transport processes are governed by the heat diffusion and energy conservation laws. Under this assumption, the heat flow will be directed toward the rear cold side of the sample where, after a certain time, a temperature fluctuation will occur [15]. The intensity and time evolution of such a fluctuation provide information on the initial amount of energy absorbed by the lattice. If the volume onto which that energy has been deposited is known, an estimate of the average initial ion temperature is obtained.

In order to put to test our approach, we have constructed a specific experimental setup [Fig. 1(a)] comprising a custom homemade IR pyrometer, a Ti:sapphire laser, and a sample holder mounting an optically polished stainless steel foil (AISI grade 304, thickness 5 ± 1 μm, lateral dimensions about 2×3 cm^2). The pyrometer, equipped with an InGaAs amplified sensor ($\varnothing = 1$ mm), was operated within the 1700–2500 nm wavelength window, thus, being sensitive to blackbody radiative emission above about 500 K. In order to accurately measure the temperature in this regime, the sample foil was heated up to a base temperature, T_0 (around 580 K), by a couple of resistive heaters installed on the sample holder. The IR pyrometer was positioned and aligned to monitor the rear side of the sample and detect the temperature fluctuation subsequent to the laser shot. The sensitive area of the IR pyrometer was

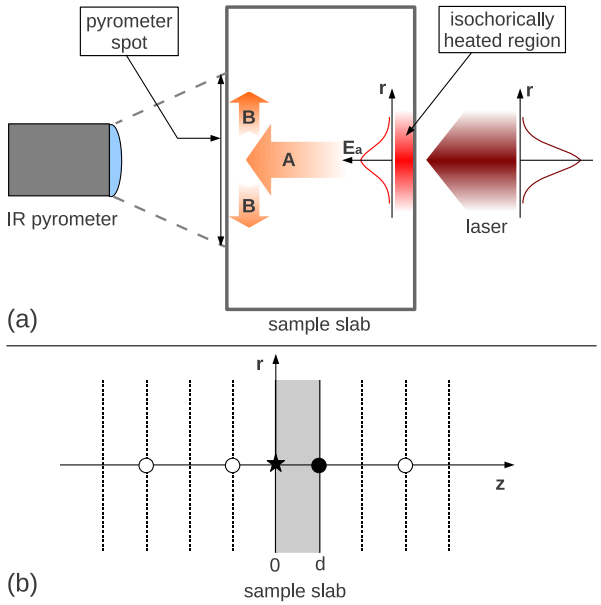

FIG. 1 (color online). (a) Sketch of the experiment. (b) Schematic description of the "image sources" method applied to an infinite sample slab. The locations of the real source (•) and the pyrometer detection center (⋆) as well as the nearest image sources (∘) are indicated.

a circle of a diameter of 250 μm. The laser operating at 800 nm was set to deliver 200 fs photon pulses. The laser beam has been focused on the sample foil to form a Gaussian spot with a FWHM of about 70 micron and with "s" polarization.

We present the results of three representative sets of measurements performed with the laser pulse energy (E_p) at 2.9, 2.0, and 1.2 mJ. An oscilloscope, triggered with the laser, has been used to record the voltage response of the pyrometer. The sample has been hit by a single laser pulse and then moved in a position contiguous to the damaged point. This procedure has been repeated 20 times for each energy, then the pyrometer temporal voltage profiles have been averaged, thus, obtaining the data shown in Fig. 2. The time scale for the temperature fluctuation extends over the millisecond time domain, thus, suggesting that a relatively slow energy transfer process, compatible with heat diffusion, governs the observed phenomenon.

In order to gain quantitative insight from the data, in the spirit of the approach in our previous paper [16], we have developed a specific theoretical model based on the classical heat diffusion law. In the general case of a homogeneous isotropic medium, the solution of the heat equation for a singular initial condition, $\delta(t)\delta(\vec{r} - \vec{r}_0)$, is a 3D Gaussian function centered at $\vec{r}_0$ with variance $\sigma^2 = 2Dt$, where D is the thermal diffusivity of the sample. For stainless steel, with $D \approx 5 \times 10^{-6}$ m^2/s, we expect that after 100 ms, one obtains $\sigma \approx 1$ mm. Therefore, we can realistically assume that in our experiment the sample region affected by the heat diffusion is fully contained within the lateral sample size. Under this assumption, we are enabled to model our sample as an infinite slab of stainless steel confined between the two planes $z = 0$ and $z = d$, where $d = 5$ μm.

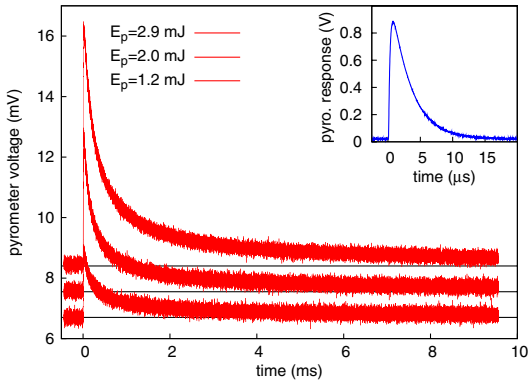

FIG. 2 (color online). IR pyrometer voltage signals recorded on the rear side of the stainless steel slab (thickness: 5 μm) as a function of time after absorption of a 200 fs laser pulse on the front side. Measurements have been carried out at three different laser pulse energies (E_p): 2.9, 2.0, and 1.2 mJ. The curves for $E_p = 2.0$ mJ and $E_p = 1.2$ mJ have been shifted, respectively, by -0.4 and -1.2 mV to ameliorate readability of the figure. The pyrometer response function for a delta-like excitation is shown within the inset.

For this geometry, we can exploit the method of the image sources (or the "method of images," described, for example, in Ref. [17]) to analytically calculate the solution of the heat equation for a 3D sample. In this theoretical scheme, the center of the heat source coincides with the center of the laser beam at the surface $z = d$ of the sample. An infinite number of equally spaced imaginary sources, positioned at $(0, 0, \pm nd)$ as depicted in Fig. 1(b), guarantees appropriate boundary conditions, i.e., the absence of heat flux through the planes $z = 0$ and $z = d$. The center of the pyrometer spot is positioned at the $(0, 0, 0)$ point.

The general solution for the heat diffusion in an infinite slab is then given by a series of 3D time-dependent Gaussians centered at equally spaced points:

$$f(\vec{r}, t) = \frac{e^{-[(x^2+y^2)/2(2Dt)]}}{2\pi(2Dt)} \times \sum_{n(\text{odd})=1}^{\infty} \frac{e^{-[(z-nd)^2/2(2Dt)]} + e^{-[(z+nd)^2/2(2Dt)]}}{[2\pi(2Dt)]^{(1/2)}}. \quad (1)$$

A Gaussian laser beam is likely to produce, on the struck side of a linearly absorbing medium, a Gaussian distribution of deposited energy. Accordingly, we assume that the initial, $(t = 0)$, energy density profile on the $z = d$ plane is described by a function, $\mathcal{E}(\vec{r}) = g(x, y)\delta(z - d)$, where $g(x, y)$ is a Gaussian of integral $2E_a$ (E_a being the total absorbed energy in the real sample slab) and standard deviation, s. With this initial condition, the general solution for the heat diffusion on the plane $z = 0$ is given by the convolution of Eq. (1) with $g(x, y)$, thus, leading to this space-time dependence of the excess temperature on the rear sample surface:

$$\Delta T(r, t) = \frac{2E_a}{c\rho} \frac{e^{-[r^2/2(2Dt+s^2)]}}{2\pi(2Dt + s^2)} \sum_{n(\text{odd})=1}^{\infty} \frac{2e^{-[n^2d^2/2(2Dt)]}}{[2\pi(2Dt)]^{(1/2)}}, \quad (2)$$

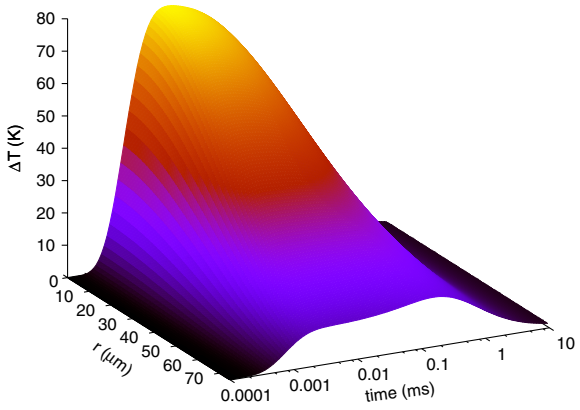

FIG. 3 (color online). Simulated temperature profile [Eq. (2), $E_a = 15.8$ μJ, $s = 38$ μm] on the rear side of a stainless steel foil, as a function of time and radial distance from the center of the laser axis.

where we exploited the radial symmetry of the system ($r = \sqrt{x^2 + y^2}$). At $t \approx 0$, only the $n = 1$ term in the series of Eq. (2) gives a tangible contribution; therefore, the time dependence reflects a 1D diffusion process (being $2Dt + s^2 \gg 2Dt$), as represented by the arrow "A" in Fig. 1(a). In the long time approximation ($2Dt \gg d^2$), many terms have to be considered and the series can be approximated by an integral of value $1/2d$, then the resulting long time temporal dependence in Eq. (2) is that associated with a 2D diffusion process through the slab side indicated by the arrows "B" in Fig. 1(a). Figure 3 shows the space-time temperature variation, $\Delta T(r, t)$ [Eq. (2)], on the rear side of the sample after absorption of 15.8 μJ of energy deposited by a Gaussian pulse ($s = 38$ μm). $\Delta T(r, t)$ has been calculated using recommended parameters for stainless steel 304 at 600 K: $D = 4.5 \times 10^{-6}$ m^2/s, $\rho = 7780$ kg/m^3, and $c = 550$ J/(kg K) [18,19].

For the temperature calibration, we adopted an empirical function that reflects the exponential dependence (Wien law) of the IR detector output voltage on the temperature:

$$V(T) = V_0 + K \exp\left(-\frac{T_\lambda}{T}\right), \quad (3)$$

with dark voltage $V_0 = 5.0$ mV, $K = 407$ V, and $T_\lambda = 6851$ K. The pyrometer sensitive area was approximated by a circular spot of radius R. For small times, the pyrometer will probe a nonhomogeneous temperature profile (see Fig. 3) and the total current on the photodiode (and resulting amplified voltage output) will reflect a surface average of the calibration curve expressed, in circular symmetry, by

$$V(t) = \frac{1}{R^2} \int_0^R V(T_0 + \Delta T(r, t))2rdr. \quad (4)$$

Equation (4) finally provides a theoretical curve suitable to model the experimental data presented in Fig. 2. The function, $V(t)$, has been convoluted with the detector

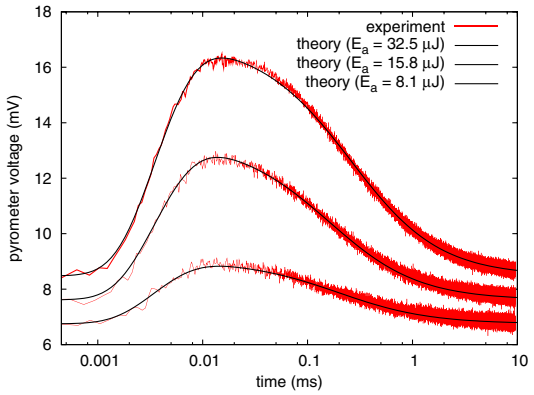

FIG. 4 (color online). The pyrometer voltage shown in Fig. 2 for 3 different laser fluences is fitted by the theoretical curve $V(t)$ (details within the text). The curves for $E_a = 15.8$ μJ, and $E_a = 8.1$ μJ have been shifted, respectively, by -0.4 and -1.2 mV to ameliorate readability of the figure.

TABLE I. Summary of the principal parameters for the three sets of measurements carried out: nominal laser irradiance calculated for a spot of 70 μm FWHM (I), energy of laser pulses (E_p), energy effectively absorbed by the sample lattice (E_a), standard deviation of the absorbed Gaussian energy distribution (s), absorbed energy density (ϵ_a), base temperature of the sample (T_0), and maximum ion temperature ($T_{\max}$).

I (W/m^2)	E_p (mJ)	E_a (μJ)[a]	E_a/E_p (%)	s (μm)[a]	ϵ_a (J/m^2)	T_0 (K)[a]	$T_{\max}$ (eV)
1.6×10^{18}	1.2	8.1 ± 1.0	0.7	38 ± 3	893	581 ± 5	0.36 ± 0.10
2.6×10^{18}	2.0	15.8 ± 1.0	0.8	38 ± 3	1737	582 ± 5	0.70 ± 0.20
3.8×10^{18}	2.9	32.5 ± 2.0	1.1	54 ± 5	1774	589 ± 5	0.72 ± 0.20

[a]Obtained from data fitting procedure [Eq. (4), Fig. 4].

time response function (inset of Fig. 2) in order to account for the finite rise time of the InGaAs amplified sensor (about 0.7 μs at 40 dB). An excellent fit of the experimental voltage curves (Fig. 4) has been obtained by tuning the E_a, s, and T_0 parameters within a reasonable range of values. The sample thickness parameter ($d = 5$ μm), the pyrometer spot radius ($R = 50$ μm), as well as the thermodynamic parameters D, ρ, and c have been kept fixed.

Table I summarizes the results. We observe that just a small fraction ($\approx 1\%$) of the total laser pulse energy is finally absorbed by the ion system of the sample. Moreover, data indicate a raising trend of the percentage of absorbed energy upon increasing the laser pulse energy. These findings are in fair agreement with the data shown in Ref. [8]. We notice that the s parameter value at the maximum irradiance is greater than in the other two cases and substantially exceeds the expected value, being the standard deviation of the laser Gaussian spot around 30 μm. Consequently, the absorbed energy density, [$\epsilon_a = E_a/(2\pi s^2)$], does not increase linearly. We believe this is an indication that the energy absorption is approaching a saturation level. A broader Gaussian mimics the expected occurrence of a flattop absorbed energy distribution. The maximum average temperature reached by the ion system can be estimated from ϵ_a and the thickness, l, effectively heated by the laser: $T_{\max} = \epsilon_a/(c\rho l)$. A realistic estimate from the literature is $l \simeq 50$ nm [20,21]. This leads to ion temperatures in the order of tenth of eV (see Table I), compatible, for instance, with electron temperatures of FEL-heated Al ($T_e = 1.1$ eV for $I \simeq 10^{18}$ W/m^2) [11]. The ion temperature value at the maximum laser fluence is probably underestimated and less reliable than for the other cases, as it is affected by the previously discussed saturation effect not accounted by our simplified Gaussian model. We also point out that the parameter, R, used in the fitting procedure is definitely smaller than expected by about 60%. This discrepancy can be attributed to experimental systematic errors such as those affecting the sample thickness (20% uncertainty). A thinner slab (smaller d value), for instance, leads to greater R values. Moreover, uncertainty on the empirical calibration function $V(T)$ [Eq. (3)] can directly affect the R value through Eq. (4). Substantial improvement in the calibration accuracy can be achieved by using a "2-wavelength" pyrometer (see, for example, [22]).

In conclusion, we have demonstrated that it is actually possible to determine with good accuracy the amount of energy (E_a) absorbed by the ion lattice in high-energy density ultrafast experiments on solid samples. The ion temperature can be estimated from the knowledge of the volume directly heated by the laser. Additional measurements, not shown here, have confirmed that the method is robust and reliable under different experimental conditions obtained, for example, by varying the laser intensities or pyrometer spot diameters [23]. In our approach, the sample acts as a natural transducer that converts the optical energy into heat and stretches the temperature pulse duration from the picosecond domain to the millisecond one, allowing for a precise evaluation of E_a. Our strategy is to exploit these effects to our advantage in order to gain the information we need without complex additional set up and experimental data treatment. The theoretical framework for interpretation involves analytical solution of the heat diffusion equation with appropriate boundary conditions (image sources), numerical one-dimensional integrations for the pyrometer voltage, and time responses and, possibly, for non-Gaussian deposited energy profiles, and can be applied to a broad variety of solid slab specimens. This work is based on a methodology analogous to the one described in a previous simulation work for the case of very thin samples uniformly heated by an ultrashort FEL pulse [16] and can be regarded as a first experimental validation of the principle. Finally, we believe that the method described in this Letter, can successfully meet the raising demand for valid diagnostic tools essential to characterize laser generated WDM and to boost advances in this critical field of research.

This work has been carried out in the framework of the TIMEX Collaboration (TIme-resolved studies of Matter under EXtreme and metastable conditions) aimed to develop an end-station at the Fermi@Elettra FEL facility in Trieste, a project financed by the ELETTRA synchrotron radiation facility in Trieste. C. M. acknowledges support from the European Research Council under the European Community Seventh Framework Program (FP7/2007-2013)/ERC IDEAS Contract No. 202804.

*emiliano.principi@elettra.trieste.it

[1] J. J. Fortney, S. H. Glenzer, M. Koenig, B. Militzer, D. Saumon, and D. Valencia, Phys. Plasmas **16**, 041003 (2009).

[2] N. Nettelmann, R. Redmer , and D. Blaschke, Phys. Part. Nucl. **39**, 1122 (2008).

[3] J. Osterholz, F. Brandl, T. Fischer, D. Hemmers, M. Cerchez, G. Pretzler, O. Willi, and S. J. Rose, Phys. Rev. Lett. **96**, 085002 (2006).

[4] M. C. Downer, H. Ahn, D. H. Reitze, and X. Y. Wang, Int. J. Thermophys. **14**, 361 (1993).

[5] R. W. Lee *et al.*, J. Opt. Soc. Am. B **20**, 770 (2003).

[6] R. R. Fäustlin *et al.*, Phys. Rev. Lett. **104**, 125002 (2010).

[7] J. Lindl, Phys. Plasmas **2**, 3933 (1995).

[8] M. Cerchez, R. Jung, J. Osterholz, T. Toncian, O. Willi, P. Mulser, and H. Ruhl, Phys. Rev. Lett. **100**, 245001 (2008).

[9] K. H. Benneman, J. Phys. Condens. Matter **16**, R995 (2004).

[10] J. Hohlfeld, S.-S. Wellershoff, J. Güdde, U. Conrad, V. Jähnke, and E. Matthias, Chem. Phys. **251**, 237 (2000).

[11] S. M. Vinko *et al.*, Phys. Rev. Lett. **104**, 225001 (2010).

[12] G. Gregori, S. H. Glenzer, K. B. Fournier, K. M. Campbell, E. L. Dewald, O. S. Jones, J. H. Hammer, S. B. Hansen, R. J. Wallace, and O. L. Landen, Phys. Rev. Lett. **101**, 045003 (2008).

[13] A. L. Kritcher *et al.*, Science **322**, 69 (2008).

[14] S. H. Glenzer and R. Redmer, Rev. Mod. Phys. **81**, 1625 (2009).

[15] A. Mandelis, Phys. Today **53**, 29 (2000).

[16] E. Principi, C. Ferrante, A. Filipponi, F. Bencivenga, F. D'Amico, C. Masciovecchio, and A. Di Cicco, Nucl. Instrum. Methods Phys. Res., Sect. A **621**, 643 (2010).

[17] H. S. Carslaw and J. C. Jaeger, *Conduction of Heat in Solids* (Oxford University, Oxford, 1959).

[18] J. Jensen *et al.*, *Selected Cryogenic Data Notebook* (Brookhaven National Laboratory, Associated Universities, Inc., Upton, NY, 1980).

[19] R. H. Bogaard, P. D. Desai, H. H. Li, and C. Y. Ho, Thermochim. Acta **218**, 373 (1993).

[20] S. Nolte, C. Momma, H. Jacobs, A. Tünnermann, B. N. Chichkov, B. Wellegehausen, and H. Welling, J. Opt. Soc. Am. B **14**, 2716 (1997).

[21] P. Mannion, J. Magee, E. Coyne, and G. M. O'Connor, Proc. SPIE Int. Soc. Opt. Eng. **4876**, 470 (2003).

[22] D. Hernandez, A. Netchaieff, and A. Stein, Rev. Sci. Instrum. **80**, 094903 (2009).

[23] See Supplemental Material at http://link.aps.org/supplemental/10.1103/PhysRevLett.109.025005 for a selection of additional measurements.